Polymer 49 (2008) 2656–2661

Contents lists available at ScienceDirect

Polymer

journal homepage: www.elsevier.com/locate/polymer

# Thermomechanical properties of stereoblock poly(lactic acid)s with different PLLA/PDLA block compositions

Masayuki Hirata, Yoshiharu Kimura*

*Department of Biomolecular Engineering, Kyoto Institute of Technology, Matsugasaki, Sakyo-ku, Kyoto 606-8585, Japan*

ARTICLE INFO

*Article history:*
Received 1 February 2008
Received in revised form 4 April 2008
Accepted 7 April 2008
Available online 12 April 2008

*Keywords:*
Poly(L-lactic acid)
Stereoblock polylactide
Solid-state polycondensation

ABSTRACT

Stereoblock poly(lactic acids) (sb-PLAs), having abundant enantiomeric compositions of poly(L-lactic acid) (PLLA), were successfully synthesized by solid-state polycondensation (SSP) of the melt blends of medium molecular weight prepolymers: both PLLA and poly(D-lactic acid) (PDLA) that had primarily been prepared by melt-polycondensation. The molecular weight of the resultant PLLA-rich sb-PLA was effectively enhanced by the dehydrative coupling of abundant PLLA molecules followed by the increase in homo-chiral crystallinity. These sb-PLA were successfully fabricated into polymer films by solution casting to analyze their crystalline morphology and properties. Both DSC and WAXS revealed preferential stereocomplexation in spite of concomitant homo-chiral crystallization for these sb-PLA. Particularly, exclusive sc crystallization was observed with melt-quenched sb-PLA represented whose PDLA ratio was above 15%. Therefore, the stereoblock structure can suppress the homo-chiral crystallization and increase the sc crystallinity even with the non-equivalent PLLA/PDLA compositions. Their thermal resistivity up to 200 °C was supported by the dynamic mechanical analysis of the sb-PLA films.



## 1. Introduction

There has been growing concern about poly(L-lactic acid) (PLLA) because of its bio-based and sustainable nature. Application of PLLA, however, has been limited until now because its thermal stability is not as high as that of the conventional oil-based polymers such as poly(ethylene terephthalate) (PET). Therefore, much effort has been paid to the thermal stabilization of PLLA by controlling its crystallization behavior.

On the other hand, stereocomplex-type PLA (sc-PLA) consisting of both PLLA and its enantiomer, poly(D-lactic acid) (PDLA), has been expected to be a potentially high-performance polymer, because it shows its melting temperature ($T_m$) at 230 °C, which is 50 °C higher than that of PLLA [1]. Polymer blend of high-molecular weight PLLA and PDLA, however, is likely to form homo-chiral (hc) crystals of each polymer rather than the stereocomplex (sc) crystals [2–4]. As a way to improve the sc formation, block copolymers of PLLA and PDLA, i.e., stereoblock poly(lactic acid)s (sb-PLAs), have been developed [5–11]. The placement of the enantiomric segments of PLLA and PDLA in the neighborhood can effectively promote the sc formation [12]. The sb-PLA thus developed, however, could not be processed into fibers and films because of their relatively low molecular weight, not exceeding 100 kg/mol. Recently, we demonstrated that sb-PLA having a molecular weight higher than 100 kg/mol can be synthesized by solid-state polycondensation (SSP) of a mixture of PLLA and PDLA with medium molecular weight [12,13]. Even with this sb-PLA, fabrication of self-supported fibers and films was not possible, and the mechanical properties of the sb-PLA products remained unclarified. In this study, we optimized the SSP of the PLLA/PDLA mixture at different compositions in order to obtain sb-PLA products having enough high-molecular weight for processing, and with which polymer films were fabricated and subjected to thermomechanical analyses. In our former studies, it was revealed that at an equivalent PLLA/PDLA composition the molecular weight of the resultant sb-PLA remained less than 100 kg/mol, while at composition deviating from 1:1 ratio the higher molecular weight was attained [14]. So, we optimized the SSP at the PLLA-rich compositions as shown in Scheme 1, where the chain extension of the rich components can be driven with the increased crystallization of the elongated PLLA sequences to give high-molecular weight sb-PLAs with film-forming ability. Consequently, the thermomechanical behavior of the sb-PLA was analyzed in relation with their PLLA/PDLA composition.

## 2. Experimental

### 2.1. Materials

L-Lactic acid (99.3%e.e.: $L/D = 99.65/0.35$) was supplied as a 90 wt.-% aqueous solution by Wako Pure Chemical Industries Ltd.

* Corresponding author. Tel.: +81 75 724 7804; fax: +81 75 712 3956.
*E-mail address:* ykimura@kit.ac.jp (Y. Kimura).

0032-3861/$ – see front matter © 2008 Elsevier Ltd. All rights reserved.
doi:10.1016/j.polymer.2008.04.014

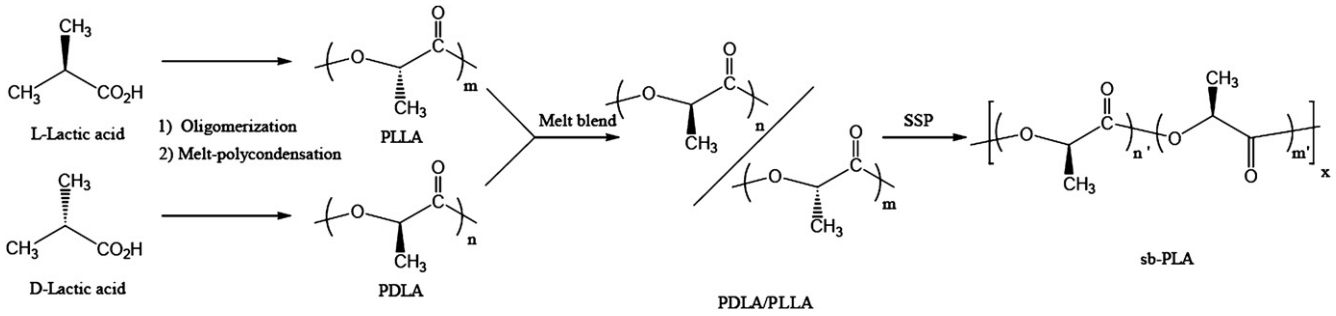


**Scheme 1.** Synthesis of sb-PLA with high-molecular weight by solid-state polycondensation (SSP) of the melt blend (PLLA/PDLA).

(Tokyo). D-Lactic acid (99.1%e.e.: $L/D = 99.55/0.45$) was supplied as a 90 wt.-% aqueous solution by Musashino Chemical Laboratory Ltd. (Tokyo). Stannous dichloride dihydrate ($SnCl_2 \cdot 2H_2O$) and *p*-toluenesulfonic acid monohydrate (TSA) were purchased from Nacalai Tesque Co. (Kyoto). 1,1,1,3,3,3-Hexafluoro-2-propanol (HFIP) was received from Central Glass Co. Ltd. (Yamaguchi). All the chemicals were used as received. The PLLA and PDLA having medium molecular weights were synthesized as reported previously [14]. In short, both oligo(L-lactic acid) (OLLA) and oligo(D-lactic acid) (ODLA) having a degree of polymerization (DP) of 5–8 were prepared in large scale by dehydration of 90 wt.-% aqueous solutions of L- and D-lactic acids, respectively. Each of OLLA and ODLA (50 g) was mixed with $SnCl_2 \cdot 2H_2O$ (0.05 g) and TSA (0.05 g) and heated at 180 °C by reducing the pressure to $13.3 \times 10^2$ Pa. On reaching $13.3 \times 10^2$ Pa, the heating was further continued for 3–5 h. At the end of the reaction, PLLA and PDLA with $M_w = 40$–50 kg/mol were obtained as white solid [15–17].

### 2.2. Measurements

A Shimadzu DSC-60 thermal analyzer was used for analyzing the thermal properties of polymer samples with α-alumina as the reference under a nitrogen atmosphere. The samples were heated from 30 to 240 °C at a heating rate of 20 °C min (the 1st heating scan). Then the samples were quenched in liquid $N_2$, heated from 30 to 250 °C (the 2nd heating scan), and cooled down to 50 °C at a rate of −10 °C/min (cooling scan). They were finally heated from 30 to 250 °C (the 3rd heating scan).

WAXS was recorded on a Rigaku 2100 FSL X-ray diffraction system with a Rigaku RINT 2000 X-ray generator operated at 40 kV and 50 mA using nickel-filtered Cu Kα radiation of a wave length of 0.1542 nm in a $2\theta$ range of 5°–40° at a scan rate of 2° $min^{-1}$.

500 MHz $^1H$ and 125 MHz $^{13}C$ NMR spectra were measured on a Bruker ARX spectrometer with samples dissolved in deuterated chloroform ($CDCl_3$) containing 1 vol-% tetramethylsilane as the internal reference. Although the as-prepared sb-PLA reprecipitated from its dichloromethane/HFIP solution also became soluble in it, addition of a few drops of HFIP in the chloroform solution gave a clear solution of sb-PLA, with which the NMR measurement was conducted.

The number- ($M_n$) and weight-average ($M_w$) molecular weights were determined by the size exclusion chromatography (SEC) with a Shimadzu analyzer system comprising LC-10ADvp pump, a RID-10A refractive index detector, and a C-R7A Chromatopac data processor. HFIP containing 1 mol.-% sodium trifluoroacetate was eluted at 40 °C through a styrene-divinylbenzene copolymer gel column (Shodex HFIP-806, 8.0 mm inner diameter × 300 mm length). The molecular weights were calibrated with poly(methyl methacrylate) (PMMA) as the standards.

Dynamic mechanical analysis (DMA) was performed on a Rheologel-E 4000 analyzer (UBM Co., Ltd., Japan) operated on the tension mode at a constant frequency of 32 Hz. The experiments were carried out in a temperature range from 40 to 240 °C at a heating rate of 3 °C/min.

### 2.3. SSP of the PLLA/PDLA mixtures

Both PLLA and PDLA having medium molecular weights were pulverized, mixed in a flask at a predetermined PLLA/PDLA compositions (10.0/0, 9.5/0.5, 9.0/1.0, 8.5/1.5, 8.0/2.0 in wt.-%), and desiccated at room temperature for 2 h. Then, the powder mixture was heat-treated at 110 °C and $6.7 \times 10$ Pa for 2 h. Then, it was heated to 160–170 °C under a nitrogen atmosphere for melt-blending and well mixed under mechanical stirring for 5 min. The melt-blend obtained was then cooled down, pulverized with a grinding machine (WB-1 purchased from Osaka Chemical Company), and subjected to SSP at 13.3–26.6 Pa by raising the reaction temperature stepwise, i.e., at 140, 150 and 160 °C for each 10 h. The SSP products were sampled every 10 h passing, if necessary.

Each of the SSP products (3.0–4.0 g) obtained in powder state was stirred in an acetone solution containing a few drops of 0.2 N HCl for removing the tin catalyst from the polymer. The polymer was then dissolved in dichloromethane and reacted with two drops of acetic anhydride for the end-capping reaction of the hydroxyl terminals. The polymer was completely dissolved in the solution by adding a small amount of HFIP and reprecipitated into an excess methanol. The polymer precipitates were filtered and dried in vacuum at 60 and 80 °C for each 4 h.

### 2.4. Preparation of polymer films of sb-PLA

Each of the produced sb-PLA polymers (PLLA/PDLA = 100/0, 95/5, 90/10, 85/15, 80/20) was dissolved in a dichloromethane (95%)/HFIP (5%) mixed solvent at a concentration of 5 g/dl, stirred for 20 min, and cast into a Petri dish which had primarily been surface-treated with trichloromethylsilane to prevent adhesion of the film. After evaporation of the solvent by desiccation at room temperature for 3 h, a solidified film was peeled off from the Petri dish and dried in vacuum at 60 and 80 °C for each 4 h. The complete removal of the solvent from the film was confirmed by $^1H$ NMR spectroscopy.

## 3. Results and discussion

### 3.1. Synthesis of sb-PLA at PLLA-rich compositions

PLLA and PDLA having medium molecular weights were primarily prepared by melt-polycondensation of OLLA and ODLA, respectively, with the binary catalyst $SnCl_2$/TSA. Their molecular weights were controlled at $M_w = 45$ kg/mol ($M_w/M_n = 1.5$) for PLLA and $M_w = 57$ kg/mol ($M_w/M_n = 1.5$) for PDLA. Both polymers were melt-blended at the PLLA-rich compositions: PLLA/PDLA = 100/0,

95/5, 90/10, 85/15, 80/20 (in wt.-%). This melt-blending could be conducted at 170 °C because the starting PLLA and PDLA with medium molecular weights were allowed to melt around 150–160 °C and little stereocomplexation was induced at the present PLLA-rich compositions. At this processing temperature thermal degradation and depolymerization of the PLLA and PDLA were successfully minimized. The melt-blends were then cooled down and subjected to SSP where the reaction temperature was raised stepwise from 140 to 160 °C as described in Section 2. The PLLA-rich melt-blends and SSP products obtained are denoted as L-MB*X* and L-SB*X*, respectively, where *X* denotes the PLLA composition used for melt-blending. Tables 1 and 2 summarize the results of the melt-blending and SSP, respectively. The polymer recoveries of the L-MB*X* decreased to 82% in some cases, because the lactide formed during the melt-blending was evaporated during the heat treatment. The final polymer recoveries of L-SB*X* also decreased to a level of 81–87% depending on the amount of lactide formation. While the $M_w$ values of the melt-blends were almost comparable to each other, those of the SSP products increased with increasing the reaction temperature or time. With this increase in $M_w$ the polydispersity was also increased.

The average block lengths ($\nu_{av}$) of L-MB*X* and L-SB*X* were determined by their carbonyl signals as described earlier [13]. Even L-MB100, to which no PDLA had been added, exhibited a relatively low $\nu_{av}$, probably because of the racemization of the L-units occurring during the melt-blending. In the finally obtained L-SB100 and 95, the $\nu_{av}$ became significantly higher than those of the corresponding L-MB100 and 95, respectively. On the other hand, the $\nu_{av}$ values of the other L-SB*X* were almost similar to those of the starting L-MB*X*. The final $M_w$ of L-SB*X* became higher with increasing *X* value (PLLA composition) and reaction time of SSP. Even for L-SB80, having the highest PDLA composition in this experiment, the $M_w$ exceeded 160 kg/mol that was enough for preparing a self-supported polymer film.

### 3.2. Thermal properties of PLLA-rich melt-blends and sb-PLA

Fig. 1 shows the DSC curves of the L-SB*X* finally obtained at 160 °C (solid line) as compared with those of their starting L-MB*X* (dotted line). While L-MB100, consisting only of PLLA, showed a sole endothermic peak at 160 °C, the other L-MB*X* showed two broad endothermic peaks around 150 °C (±10 °C) and 200 °C due to the crystal fusions of the hc and sc crystals, respectively. Their peak ratio, corresponding to the hc/sc crystal ratio, decreased with increasing PDLA composition. The L-SB*X* obtained after SSP showed completely different thermal nature. L-SB100, consisting only of PLLA, showed a single endothermic peak at 170 °C which was much higher than that of its starting L-MB100 because of the increased molecular weight or $\nu_{av}$. The other L-SB*X* containing PDLA showed two endothermic peaks, similarly to the corresponding L-MB*X*. However, the peak due to the fusion of hc crystals shifted to a temperature higher than 170 °C and became much sharper. The endothermic peak due to the fusion of sc crystals also appeared at higher temperatures (above 210 °C) than those of the corresponding L-MB*X* with little change in the peak size. These data suggest that the hc crystallinity of the reactants was allowed to increase without changing the sc crystallinity during SSP. The hc and sc crystallinities were calculated from the intensities of the two endotherms referring to the theoretical heat of fusions of hc (93 J/g) [18] and sc (142 J/g) [19] crystals previously reported. The thermal data for each L-SB*X* obtained after different reaction time of SSP are summarized in Table 2. It is evident that the $T_m$ of hc crystals steadily increased to nearly 175 °C in the course of SSP although the $T_m$ of sc crystals didn't change after the first 10 h of SSP.

Fig. 2 shows the changes in hc and sc crystallinities as a function of PLLA composition (*X*) for both the starting L-MB*X* and the finally obtained L-SB*X*. The hc crystallinity decreased with decreasing *X*, while the sc crystallinity increased with it. At the identical PLLA compositions, the hc crystallinity of L-SB*X* was much larger than

**Table 1**
Typical results of melt-blending of PLLA and PDLA with medium molecular weight

| Code | Polymer recovery, % | $M_w$[a], 10 kg/mol | $M_w/M_n$[a] | $T_{mh}$[b,c], °C | $T_{ms}$[b,c], °C | $\Delta H_{mh}$[b,d], J/g | $\Delta H_{ms}$[b,d], J/g | $\nu_{av}$[e] |
|---|---|---|---|---|---|---|---|---|
| L-MB100 | 97.4[f] | 4.5 | 1.5 | 160.8 | – | 52.9 | – | 35.7 |
| L-MB95 | 82.0 | 4.4 | 1.5 | 143.5 | 197.3 | 40.1 | 3.7 | 45.4 |
| L-MB90 | 82.8 | 4.8 | 1.5 | 148.0 | 202.9 | 41.2 | 10.1 | 46.1 |
| L-MB85 | 87.9 | 4.7 | 1.5 | 144.2 | 201.8 | 36.7 | 19.8 | 41.6 |
| L-MB80 | 93.1 | 3.9 | 1.4 | 138.2 | 200.1 | 29.0 | 27.0 | 35.8 |

[a] Determined by SEC relative to PMMA standards with HFIP as the eluent (40 °C).
[b] Measured by DSC at a heating rate of 20 °C/min.
[c] $T_{mh}$ and $T_{ms}$ denote the melting temperatures of hc and sc crystals.
[d] $\Delta H_{mh}$ and $\Delta H_{mc}$ show the heats of fusion of hc and sc crystals.
[e] Determined by $^{13}C$ NMR spectra.
[f] After the thermal treatment at 110 °C and 0.5 torr for 2 h.

**Table 2**
Typical results of SSP of the melt-blends L-MB*X* and thermal properties of the L-SB*X* obtained

| Code | Temperature, °C | Reaction time, h | Polymer recovery, %[a] | $M_w$, 10 kg/mol | $M_w/M_n$ | $T_{mh}$, °C | $T_{ms}$, °C | $\Delta H_{mh}$, J/g | $\Delta H_{ms}$, J/g | $\nu_{av}$ |
|---|---|---|---|---|---|---|---|---|---|---|
| L-SB100 | 140 | 10 | – | 7.1 | 1.5 | 159.1 | – | 60.7 | – | – |
| | 150 | 20 | – | 18.0 | 2.4 | 170.4 | – | 65.0 | – | – |
| | 160 | 30 | 84.0 | 25.0 | 2.5 | 171.9 | – | 72.8 | – | 73.5 |
| L-SB95 | 140 | 10 | – | 7.3 | 1.5 | 160.8 | 207.3 | 55.5 | 2.7 | – |
| | 150 | 20 | – | 20.0 | 2.1 | 176.2 | 208.1 | 60.6 | 2.8 | – |
| | 160 | 30 | 81.0 | 35.0 | 2.4 | 175.4 | 209.1 | 68.7 | 2.6 | 62.6 |
| L-SB90 | 140 | 10 | – | 7.0 | 1.5 | 166.8 | 209.6 | 48.8 | 8.6 | – |
| | 150 | 20 | – | 14.0 | 1.8 | 171.8 | 209.6 | 57.0 | 7.9 | – |
| | 160 | 30 | 82.5 | 23.0 | 2.0 | 174.2 | 209.2 | 62.9 | 9.7 | 42.5 |
| L-SB85 | 140 | 10 | – | 6.3 | 2.5 | 167.3 | 209.8 | 45.4 | 14.5 | – |
| | 150 | 20 | – | 18.0 | 2.1 | 173.0 | 209.8 | 51.9 | 18.4 | – |
| | 160 | 30 | 85.0 | 24.0 | 2.9 | 175.0 | 209.8 | 53.9 | 23.3 | 31.7 |
| L-SB80 | 140 | 10 | – | 6.3 | 1.5 | 161.3 | 209.9 | 39.7 | 21.2 | – |
| | 150 | 20 | – | 10.0 | 1.9 | 169.2 | 210.6 | 40.1 | 23.9 | – |
| | 160 | 30 | 87.1 | 16.0 | 2.4 | 172.7 | 210.6 | 43.6 | 28.0 | 31.7 |

Refer to Table 1 for the other symbols and notes.
[a] After the thermal treatment at 110 °C and 0.5 torr for 2 h.

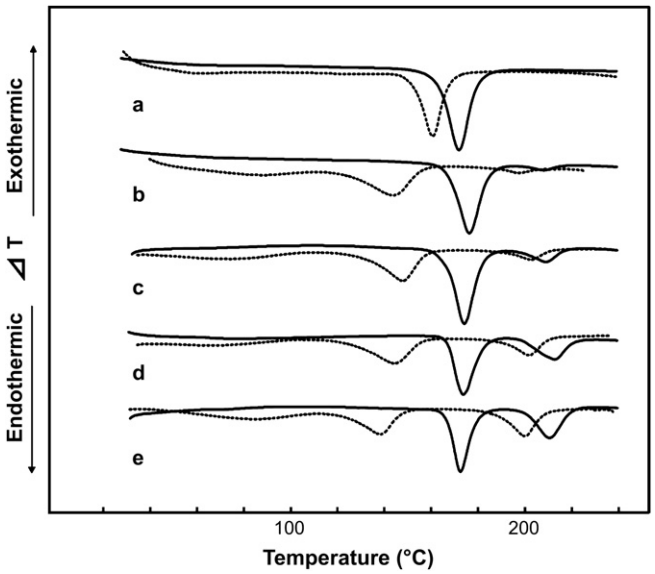


**Fig. 1.** DSC curves of L-MB*X* and L-SB*X* in the 1st scan (from 30 to 240 °C at 20 °C/min). Dotted line: (a) L-MB100, (b) 95, (c) 90, (d) 85, (e) 80; solid line: (a) L-SB100, (b) 95, (c) 90, (d) 85, (e) 80.

that of L-MB*X* by a 15/2 ratio, although the sc crystallinity remained almost identical in the both. These data strongly support the fact that the polycondensation has been induced in the abundant PLLA domain to facilitate the molecular weight increase and the simultaneous hc crystallization.

### 3.3. Characterization of L-SBX films

Each of the finally obtained L-SB*X* was fabricated into a polymer film by solution casting to investigate its structure–property relationship. Each film obtained was semi-transparent, glossy, and strong enough to be self-supported. Fig. 3 shows the WAXS profiles of the five sample films with different compositions (*X*). All the samples other than L-SB100 (PLLA homoplymer) exhibited the diffraction peaks of sc ($2\theta = 12°$, 21° and 24°) and hc crystals ($2\theta = 16.5°$ and 19°) [4,20,21]. The intensities of the latter peaks became stronger with increasing PDLA composition while those of the former peaks were weaker with it. These data reveal that both sc and hc crystallizations were promoted during the solution

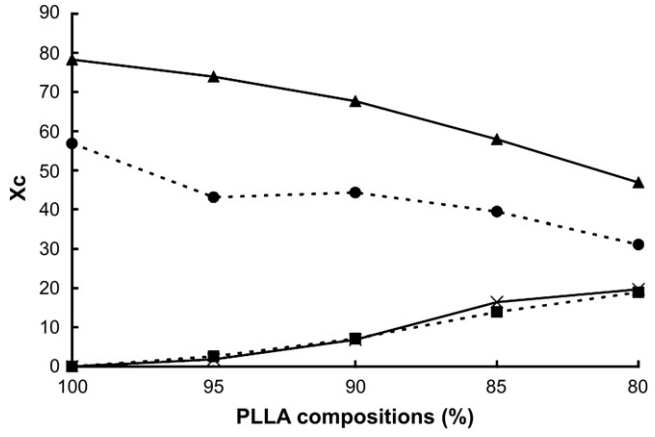


**Fig. 2.** Changes in crystallinity ($X_c$) as a function of the PLLA composition (*X*) for L-SB*X* (determined by DSC 1st scan with a heating rate of 20 °C/min). Dotted line: ● hc and ■ sc crystallinities of L-MB*X*. Solid line: ▲ hc and × sc crystallinities of L-SB*X*.

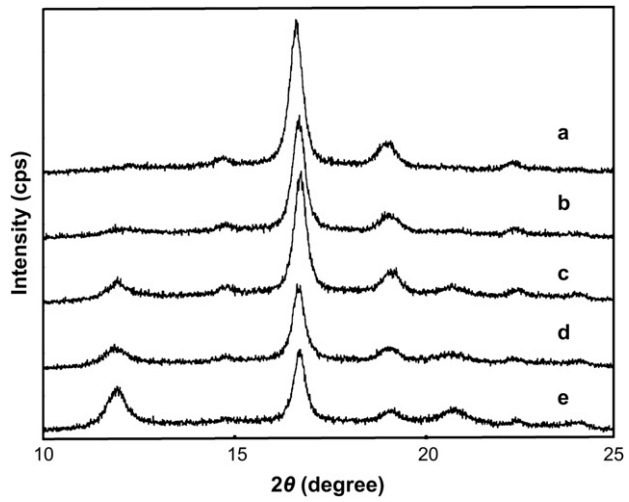


**Fig. 3.** WAXS profiles for L-SB*X* films: (a) L-SB100; (b) 95; (c) 90; (d) 85; (e) 80.

casting. The similar crystalline features were supported by DSC (data not shown).

Fig. 4 shows the DSC curves in the 2nd heating scan of L-SB*X* that were melt-quenched after the 1st heating of the film samples. Since the melt-quenched samples were glassy, they showed the crystallization above 100 °C, followed by the crystal fusion around 200 °C. In fact, L-SB95 and 90 showed a very broad crystallization exotherm as L-SB100 together with two melting endotherms at 165 and 200 °C which should be attributed to the fusion of hc and sc crystals. On the other hand, both L-SB85 and 80 exhibited a relatively sharp crystallization exotherm around 100 °C, which was much lower than that of L-SB95 and 90. The most interesting here was that only one melting endotherm was recorded around 200 °C, indicating the preferential sc crystallization over the hc crystallization. It is therefore known that the stereo-complexibility of L-SB*X* in the melt-quenching/cold crystallization process can be improved at PDLA compositions higher than 15% and that the crystallization rate is enhanced with the PDLA compositions increased.

Table 3 summarizes the thermal behaviors of the melt-quenched L-SB*X* determined from the DSC curves. The crystallization temperature ($T_{cq}$) of the hc and/or sc crystals decreased with increasing PDLA composition where $T_{cq}$ of sc crystals (105–110 °C) was known to be significantly lower than that ($T_{ch}$) of hc crystals (shown from 120 to 140 °C). The heats of crystal fusion of hc ($\Delta H_{mh}$)

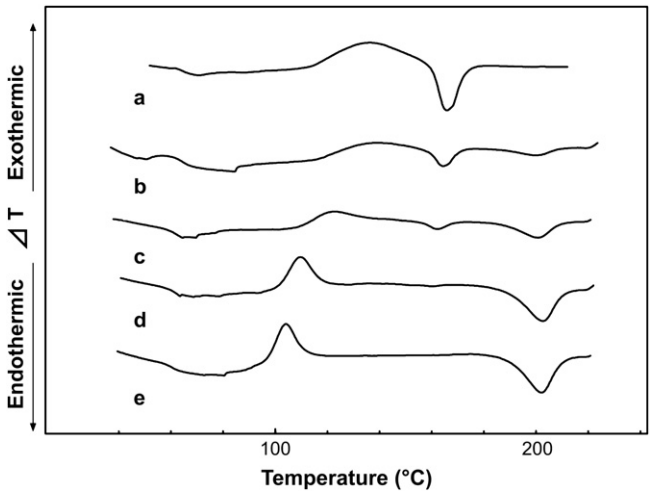


**Fig. 4.** DSC curves of L-SB*X* films in the 2nd scan (from 30 to 240 °C at 20 °C/min). (a) L-SB100; (b) 95; (c) 90; (d) 85; (e) 80.

**Table 3**
Thermal data of the melt-quenched L-SB*X* as determined by DSC 2nd heating scan[a]

| Code | $T_g$, °C | $T_{cq}$[b], °C | $T_{mh}$, °C | $T_{ms}$, °C | $\Delta H_{cq}$[c], J/g | $\Delta H_{mh}$, J/g | $\Delta H_{ms}$, J/g |
|---|---|---|---|---|---|---|---|
| L-SB100 | 61.9 | 136.3 | 165.8 | – | – | −18.4 | – |
| L-SB95 | 59.3 | 139.0 | 164.5 | 200.0 | 8.5 | −5.3 | −3.8 |
| L-SB90 | 62.6 | 122.7 | 162.2 | 200.7 | 9.9 | −2.4 | −8.6 |
| L-SB85 | 60.4 | 109.7 | – | 202.7 | 15.9 | 0 | −16.1 |
| L-SB80 | 60.5 | 104.0 | – | 202.3 | 19.7 | 0 | −20.5 |

[a] Measured by DSC (heating rate: 20 °C/min) for the samples quenched after the 1st heating scan.
[b] $T_{cq}$ shows the crystallization temperature of hc and/or sc crystals. Refer to Table 1 for the symbols and notes.
[c] $\Delta H_{cq}$ shows the total crystallization enthalpy of hc and/or sc crystals.

and sc crystals ($\Delta H_{ms}$) showed opposite decreasing and increasing behaviors, respectively, with increasing PDLA composition, and the total heat of crystal fusion ($\Delta H_{mh} + \Delta H_{ms}$) was almost identical with the total heat of crystallization ($\Delta H_{cq}$) in each sample. Therefore, $\Delta H_{ms}$ was as same with $\Delta H_{cq}$ in L-SB85 and 80. Fig. 5 compares the changes in crystallinity as a function of the PLLA composition for the solution-cast films and their melt-quenched samples. While the sc crystallinities were comparable in both cases, the hc crystallinities were much different from each other. This fact suggests that the formation of hc crystals was significantly suppressed in the melt-quenched samples probably because the interaction of the PLLA and PDLA block chains is stronger in the melt state than in the solution state to retard the hc crystallization.

Fig. 6 shows the crystallization behaviors of L-SB*X* in the cooling process of the melt samples attained after the 2nd heating scan. L-SB100 and 95 exhibited a broad inconspicuous peak, suggesting a slow rate of crystallization. L-SB90 and 85 represented two exothermic peaks which may be attributed to the sc and hc crystallizations, although the higher temperature peak was very weak in L-SB90. L-SB80, on the other hand, showed only one exothermic peak at the higher temperature. For analyzing the crystalline states of these cooled samples, the 3rd heating scan was conducted after the cooling scan. Table 4 summarizes the thermal data obtained as compared with those of the cooling scan. In the 3rd heating scan, the heat of fusion of hc crystals ($\Delta H_{mh}$) decreased with increasing the PDLA composition, while the heat of fusion of sc crystals ($\Delta H_{ms}$) increased with it. Therefore, even L-SB80, having shown one crystallization peak in the cooling scan, formed a small amount of hc crystals. Since the heat of crystallization ($\Delta H_{cm}$) in the cooling scan jumped up above 90% in PDLA composition (L-SB90), the sc crystals first formed could nucleate the hc crystals. Therefore, the present static heating/cooling process could not allow exclusive sc crystallization even for L-SB80. We expect the exclusive formation of sc crystals when some shear is applied to the melt of L-SB80 (or L-SB*X* with PDLA composition higher than 15%) by the ordinary melt-processing.

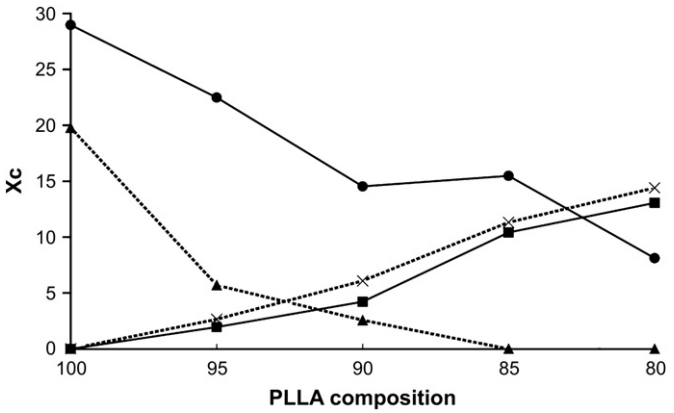


**Fig. 5.** Changes in crystallinity ($X_c$) as a function of the PLLA composition ($X$) for L-SB*X* (determined by DSC 1st and 2nd scan with a heating rate of 20 °C/min). Dotted line: ● hc and ■ sc crystallinities of L-SB*X*. Solid line: ▲ hc and × sc crystallinities in melt-quenched L-SB*X*.

### 3.4. DMA measurements of L-SBX films

Fig. 7 shows the temperature dependences of the dynamic mechanical properties of the L-SB*X* films. L-SB100 melted down around 160 °C. On the other hand, L-SB95, 90, 85, and 80 retained their storage moduli ($E'$) to a level of $10^6$–$10^7$ Pa up to 185–200 °C because of the presence of sc crystals that can resist the melt-down occurring around $T_m$ of PLLA. These results revealed that the L-SB*X* films should have much higher thermal resistance than the conventional PLLA materials [22]. The intermolecular stereocomplexation could afford cross-linking points and increase the storage modulus even after the melting of the hc crystals. Especially, L-SB85 and 80 showed higher storage moduli because of

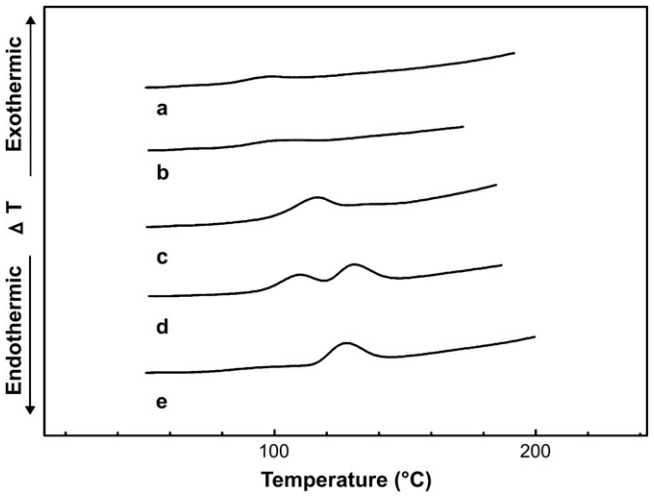


**Fig. 6.** DSC curves of L-SB*X* films in the cooling scan after the 2nd heating (from 240 to 40 °C at −10 °C/min). (a) L-SB100; (b) 95; (c) 90; (d) 85; (e) 80.

**Table 4**
Melt-crystallization of L-SB*X* analyzed by DSC 2nd cooling and the following 3rd heating scans

| Code | The cooling scan[a] | | The 3rd heating scan[b] | |
|---|---|---|---|---|
| | $\Delta H_{ch}$[c], J/g | $\Delta H_{cs}$[c], J/g | $\Delta H_{mh}$, J/g | $\Delta H_{ms}$, J/g |
| L-SB100 | 3.0 | – | 29.3 | 0 |
| L-SB95 | 1.8 | – | 23.7 | 3.6 |
| L-SB90 | 18.9 | – | 17.3 | 8.3 |
| L-SB85 | 9.9 | 12.1 | 15.8 | 16.1 |
| L-SB80 | – | 16.9 | 3.3 | 17.7 |

[a] Cooling rate: 10 °C/min.
[b] Heating rate: 20 °C/min.
[c] $\Delta H_{ch}$ and $\Delta H_{cs}$ denote the heats of crystallization of hc and sc crystals, respectively, assuming that the higher and lower exothermic peaks are attributed to the respective crystallizations. Refer to Table 1 for the other symbols and notes.

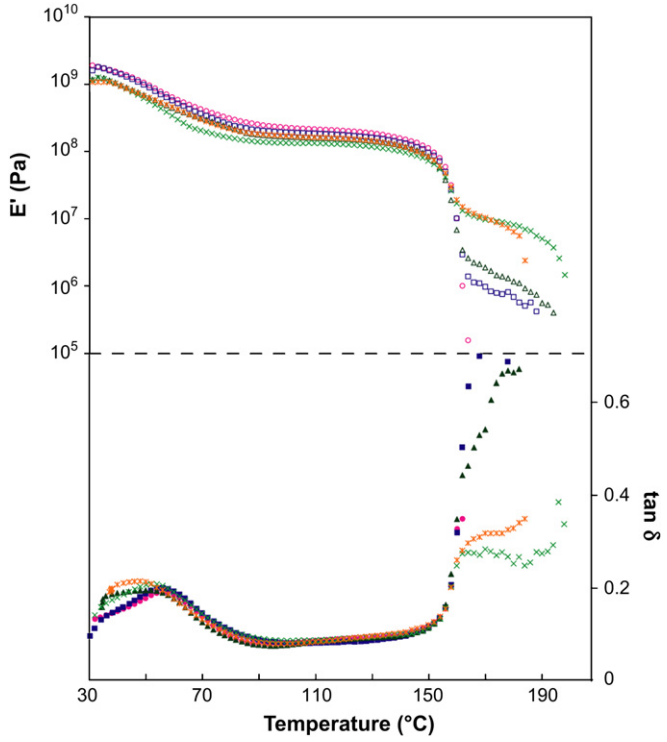


**Fig. 7.** Temperature dependences of storage modulus and tan $\delta$ for the solution-cast L-SB*X* films in MDA (from 30 to 240 °C at 3 °C/min). *E'*: ○ L-SB100 □ L-SB95 △ L-SB90 × L-SB85 * L-SB80. tan $\delta$: ● L-SB100 ■ L-SB95 ▲ L-SB90 × L-SB85 * L-SB80.

their higher involvement of the sc crystals. As shown by the changes of tan $\delta$, the $\alpha$-relaxation temperatures (around 50 °C) of L-SB85 and 80 were slightly lower than those (around 60 °C) of L-SB100 and 95. This fact may be because the free volume has been enlarged in the amorphous domain during the formation of sc crystals in the samples having high sc crystallinity.

## 4. Conclusion

The synthesis of sb-PLA having non-equivalent PDLA/PLLA composition was optimized to attain high-molecular weights that can allow fabrication of their polymer films. In this synthesis the PLLA and PDLA prepolymers having medium molecular weights were melt-blended at several PLLA-rich compositions and subjected to SSP at mild reaction temperatures to obtain L-SB*X* having average block lengths of 30–60 isotactic units depending on the PLLA compositions. The molecular weight of the L-SB*X* was found to become higher with increasing the PLLA composition. The increase in molecular weight is attributed to the dehydrative condensation of PLLA prepolymer which is abundant after the sc formation with the PDLA prepolymer as well as to the following increase in hc crystallinity. The thermal properties of the L-SB*X* depended on their PLLA composition by which the hc/sc crystal ratio was determined after a preferential stereocomplexation. The heating of the melt-quenched samples of L-SB*X* having PDLA composition higher than 15% could form sc crystals exclusively, while their melt-cooling could not help forming a small amount of hc crystals despite the high sc crystallinity attained. DMA measurements represented the retention of storage modulus above the $T_m$ of hc crystals (160 °C). Based on these data we expect that PLLA-rich sb-PLA can be applied as high-performance materials as the ordinary sc-PLA by saving the use of more expensive D-lactic acid.

## References

[1] Tsuji H, Ikada Y, Hyon SH, Kimura Y, Kitao T. J Appl Polym Sci 1994;51:337.
[2] Dorgan JR, Lehermeier H, Mang M. J Polym Environ 2000;8:1–9.
[3] Tsuji H, Ikada Y. Curr Trends Polym Sci 1999;4:27–46.
[4] Tsuji H, Hyon SH, Ikada Y. Macromolecules 1991;24:5651–6.
[5] Yui N, Dijkstra PJ, Feijen J. Makromol Chem 1990;191:481–8.
[6] Spassky N, Wisniewski M, Pluta C, Le Borgne A. Macromol Chem Phys 1996; 197:2627–37.
[7] Ovitt TM, Coates GW. J Polym Sci Part A Polym Chem 2000;38:4686–92.
[8] Ovitt TM, Coates GW. J Am Chem Soc 2002;124:1316–26.
[9] Radano CP, Baker GL, Smith III MR. J Am Chem Soc 2000;122:1552–3.
[10] Tang Z, Yang Y, Pang X, Hu J, Chen X, Hu N, et al. J Appl Polym Sci 2005;98: 102–8.
[11] Majerska K, Duda A. J Am Chem Soc 2004;126:1026–7.
[12] Fukushima K, Furuhashi Y, Sogo K, Miura S, Kimura Y. Macromol Biosci 2005; 5:21–9.
[13] Fukushima K, Kimura Y. Macromol Symp 2005;224:133–43.
[14] Fukushima K, Hirata M, Kimura Y. Macromolecules 2007;40:3049–55.
[15] Moon SI, Kimura Y. Polym Int 2003;52:299–303.
[16] Moon SI, Lee CW, Taniguchi I, Miyamoto M, Kimura Y. Polymer 2001;42: 5059–62.
[17] Moon S-I, Taniguchi I, Miyamoto M, Kimura Y, Lee C-W. High Perform Polym 2001;13:S189–96.
[18] Loomis GL, Murdoch JR, Gardner KH. Polym Prepr (Am Chem Soc Div Polym Chem) 1990;31:55.
[19] Fischer EW, Sterzel HJ, Wegner G. Kolloid Z Z Polym 1973;251:980–90.
[20] Hoogsteen W, Postema AR, Pennings AJ, Ten Brinke G, Zugenmaier P. Macromolecules 1990;23:634–42.
[21] Brizzolara D, Cantow H-J, Diederichs K, Keller E, Domb AJ. Macromolecules 1996;29:191–7.
[22] Jamshidi K, Hyon SH, Ikada Y. Polymer 1988;29:2229–34.